

The Formation Histories of Galaxy Clusters

J.D. Cohn^{a,c, 1} and Martin White^{b,c, 2}

^a*Space Sciences Laboratory, ^bDepartments of Physics and Astronomy,*

^c*Theoretical Astrophysics Center*

University of California, Berkeley, CA 94720

Abstract

A sample of hundreds of simulated galaxy clusters is used to study the statistical properties of galaxy cluster formation. Individual assembly histories are discussed, the degree of virialization is demonstrated and various commonly used formation times are measured and inter-compared. In addition, the fraction of clusters which have “recently” undergone a major merger or significant mass jump is calculated as a function of lookback time and interval. The fraction of three- and four-body mergers is also studied.

1 Introduction

Due to their immense size, galaxy clusters can be easily identified with their dark matter halos, and their clustering and number counts can be reliably predicted by dark matter simulations. However in order to find or “weigh” galaxy clusters observationally, assumptions of dynamical equilibrium and less understood astrophysics usually come into play³. Since halos form via the accretion and mergers of smaller units, and for clusters this process is occurring to the present time, such assumptions need to be specified precisely. For example, how well a galaxy cluster is described by equilibrium properties depends upon whether it has recently undergone a major merger (where “major” means disrupting equilibrium) and upon the specific methods used for its detection and mass measurement. Thus even if one is only interested in galaxy clusters as “test particles” or peaks in the density field, the history of cluster growth is

¹ jcohn@astro.berkeley.edu

² mwhite@berkeley.edu

³ Weak gravitational lensing measures mass without equilibrium assumptions, but only in projection (see e.g. Refs. (1)).

important in order to make contact with observations. Cluster growth histories are also important for understanding other cluster properties. For example, several observational phenomena (see below) are associated with clusters which have recently undergone mergers. A related question is which cluster properties have the least sensitivity to cluster assembly histories.

In this paper we study the assembly history and degree of virialization of high-mass halos in large N-body simulations. A cluster assembly history can be characterized either by events with specific occurrence times, such as mergers or large mass changes, or by properties of its entire history, e.g. a parameterization of the mass as a function of time. We calculate several such quantities for a statistically significant sample of halos. We consider several popular formation time definitions and cluster history parameterizations and statistics. We also calculate the fraction of “recently” merged galaxy clusters as a function of redshift, back to $z \sim 1$.

The definitions of both “merger” and “recently” depend on the cluster property of interest and we explore several choices. We also find the fraction of galaxy clusters which have had a recent large mass gain (including accretion) for several choices of interval and two final/initial mass ratios. Merger histories can be reliably extracted from N-body simulations, and as such these recently merged fractions are implicit in earlier work. However, it can be difficult to obtain specific numbers from the literature for Λ CDM models, especially if one has a particular relaxation time in mind. In part this is because previous studies of different quantities at different times have been published over several years, often using different cosmological models. Here we compute several of these quantities for a much larger sample than used in earlier work, for Λ CDM cosmologies, and present them in a homogeneous manner in the hope that this will be a useful reference for the community.

The outline of the paper is as follows. Section 2 is a review, including pointers to earlier work on formation times and examples of observed merger phenomena. Section 3 describes the simulations and methods. A reader interested primary in the results can skip directly to Section 4, which has comparisons and distributions of some cluster formation properties, and the fractions of clusters which have recently merged or had a large mass increase, as a function of time. Three and four-body major mergers are also studied. Finally, Section 5 presents our conclusions.

2 Background

The growth of structure by mergers and accretion is key to the hierarchical paradigm of structure formation, and thus mergers and mass gains have

been studied intensively. Previous work on cluster formation histories includes Refs. (2; 3; 4; 5; 6; 7; 8; 9). While cluster assembly is a complex and ongoing process in hierarchical models, it is often useful to have some measure of when the cluster “formed”. Refs. (5; 7; 8), each with 10-20 clusters, considered formation time definitions including the redshift, z_{jump} , of the most recent large ΔM over a short time. Both (7; 8) also found a characteristic formation time z_f associated with the entire cluster growth curve using the parameterization of Ref. (10). This parameterization works extremely well for galaxy sized halos and correlates with other properties such as concentration. For galaxy clusters, Ref. (8) introduced a generalization to help better match the more recently active formation histories of galaxy clusters. Ref. (6) had a sample similar to ours and found a “turning point” time where halos went from a quickly growing phase to a more slowly growing phase, this turning point was correlated with concentration. There are other formation times considered in the literature. For instance Ref. (11) found the average mass accretion history of halos generated by extended Press-Schechter. Ref. (7) also looked at the amount of mass gain coming from large ΔM “jumps” as fraction of cluster mass. We consider these properties and their distribution for our large sample of over 500 clusters for a ΛCDM $\sigma_8 = 0.8$ model in §4.

Our second set of results is the frequency of recent mergers and recent large mass gains for some fixed lookback time and definition of “recent.” Analytic estimates of merger rates, in many cases combined with simulations, include those by Refs. (12; 3; 5; 13) (see also the extension reported in (14)). The previous work closest to the merger counts considered here is by Ref. (5) who found the major merger distribution as a function of redshift for a system which had 11 clusters at $z = 0$ (with a merger defined as an increase in halo mass such that $M_f/M_i > 1.33$) and that of Ref. (13) which also studied the recently merged population, but for a smaller number of clusters and not in as much detail. It should be noted that merger rates and the number of clusters which have recently undergone a merger are slightly different, it is the latter we study here.

Mergers can alter X-ray temperatures, luminosities, cluster galaxy light, cluster galaxy velocities and Sunyaev Zel’dovich (SZ; Ref. (15)) “flux”⁴. Observational consequences of merging clusters of galaxies have been studied analytically and with numerical simulations, e.g. Refs. (20; 21; 7). In these, the time scale for major disturbances of clusters due to mergers seems only weakly dependent upon the impact parameter (the magnitude of the distur-

⁴ Several simulations with different heating and feedback prescriptions have found small merger induced scatter in the integrated SZ flux relation (Refs. (16; 17; 18) although there are examples where a $\sim 50\%$ increase in total SZ flux for one sound crossing has been seen (19)). Significant scatter in the mass-flux relation instead appears to be dominated by that due to line of sight projection (16).

bance has a stronger dependence, e.g. see Refs (21)). We do not consider impact parameters below. The errors induced by ignoring merger effects (on X-ray luminosities and temperatures) for cosmological parameter estimates has been considered in (22)⁵. More generally, unaccounted for mergers can disguise cluster masses and alter survey selection functions.

Observationally, some signatures of mergers can be used to flag unrelaxed clusters. For instance substructure, the presence of multiple peaks in the cluster surface density on scales larger than the constituent galaxies, has been studied extensively. Several different observational methods have been used to quantify the amount of substructure in X-ray clusters (see the review (24) and references therein). The fraction of clusters exhibiting substructure has been found to be significant in several surveys. For example, Ref. (25) visually found substructure in 41% of 208 Einstein IPC images, Ref. (26) measured the emission weighted centroid variation for 65 Einstein clusters to get a substructure fraction of 61% (see also (27) for related work) and Ref. (28) found, using three different indicators, substructure in $52 \pm 7\%$ of 470 clusters in the ROSAT all-sky survey. Substructure has also been searched for in other wave-bands. For example, substructure was detected in over 80% of 25 low richness 2dFGRS clusters ((29); see their references for other studies). Following Ref. (30), substructure has been considered as a means of constraining cosmology, e.g. in (31) using 40 Chandra clusters over a range of redshifts (see also (32) for relevant simulations). A meaningful comparison of our calculated number of “recently merged” clusters to the number of observed galaxy clusters with substructure depends on relaxation times. These times depend upon the substructure measurement in question and are still not well estimated. For instance, relatively small sub-clumps may take a different amount of time to disappear depending on their density, see (24) for further discussion.

Radio halos and radio relics have been proposed as another merger indicator (see the reviews (33) and (34)). Clusters hosting radio halos and relics tend to show other signs of merger activity, however not all clusters with other indicators of recent mergers show these radio signals. In a complete sample (35) at the NRAO VLA Sky Survey surface brightness limit, only 5% of clusters had a radio halo source and 6% had a peripheral relic source, however in clusters with X-ray luminosity larger than 10^{45} erg s⁻¹, 35% had radio halos or relics. In the ROSAT sample considered above by Ref. (28), 53 clusters of the 470 had radio halos or relics, most of these were high luminosity ($L > 4.0 \times 10^{44}$ erg s⁻¹). It has been proposed that more radio halos and relics will be found in lower mass clusters as sensitivities improve (e.g. Ref. (19)). The relaxation time for radio halos and relics is not known.

⁵ They used an analytic model (23) to get a merger history, in principle our calculations here could also be used for this purpose.

The absence of mergers (i.e. a relaxed cluster) has been suggested as a requirement for cool core clusters (e.g. Refs. (36)). The fraction of cool core clusters has been measured for various samples, e.g. Ref.(37) found with Chandra that 55% of 38 clusters in the ROSAT Brightest Cluster Sample (with $z \sim 0.15 - 0.4$) show mild cooling (associated with a cooling time less than 10 Gyr) and 34 % show signs of strong cooling (a cooling time less than 2 Gyr). There are some simulations that suggest however that mergers may help form cool galaxy cluster cores (e.g. see (38)), also 5/22 of the ROSAT cooling flow clusters have significant substructure (28).

There are many more phenomena associated with mergers which are even more complex (see Sarazin's list of questions about merging clusters of galaxies (39)). The examples of merger indicators reported above have had their occurrence rates measured in some of the largest cluster samples available.

There are some differences between mergers and any form of mass gain⁶. Clusters which have gained mass primarily via accretion might be expected to be more relaxed than those who reach the same mass via a major merger. For smaller halos those with a relatively large mass gain over a short time are more clustered than halos of the same mass but without this mass gain (41). The subset of recently merged halos, in contrast, does not appear to be so biased (42). The authors of Ref. (41) conjecture that objects in denser regions tend to have more nearby material to accumulate, resulting in a bias, while the same is not true of recent mergers.

3 Methods

To investigate these questions we used two N-body simulations run with a *TreePM* code (43). Each simulation evolved 512^3 particles in a periodic cubic box, $300 h^{-1}\text{Mpc}$ on a side, for a particle mass of $1.67 \times 10^{10} h^{-1} M_\odot$. The models had $h = 0.7$, $\Omega_m = 0.3$, $\Omega_\Lambda = 0.7$ and $\sigma_8 = 0.8, 1.0$. The two normalizations span the observationally preferred range. Outputs were dumped at equal intervals of conformal time, $\delta\tau = 100 h^{-1}\text{Mpc}$ (comoving), starting at $z = 2$.⁷ Other parameters and details of the simulations can be found in (44).

For each output groups are identified with a friends of friends algorithm (FoF;

⁶ A modified version of the PS formalism that differentiates between (instantaneous) major mergers and accretion has been developed in Refs. (40).

⁷ This is the same time interval considered by Ref. (7) and shorter than that considered by Refs. (5; 8), though the latter groups still had their time spacings well within the lower limits for a merging time scale.

(45)) using a linking length $b = 0.15$ in units of the mean inter-particle spacing. These groups correspond roughly to all particles above a density of $3/(2\pi b^3) \simeq 140$ times the background density. We did not consider other group finders, a comparison between HOP (46) and FoF merger fractions for a smaller sample was considered in (13). In that case there were both fewer recently merged clusters and fewer clusters altogether for the FoF case. See also Ref. (41) for a comparison of HOP and FoF mergers and accretion for smaller mass halos. They estimate what minimum mass fraction in accretion is robust for different group fractions and find that a 20% mass increase (for a shorter length of time and smaller halos than we consider) is outside the “noise” region for the FoF vs. HOP group finders.

For each group and output time we compute a number of properties, including the mass, velocity dispersion and potential energy of the group. All properties are computed using only group members. Masses henceforth refer to friends of friends masses M_{fov} unless otherwise stated. To get M_{200} or M_{vir} conversion is needed (47) – for a fitting formula see (48). From the simulation we find $M = 1.2 M_{200}$ at $z = 0$, and $M = 0.98 M_{200}$ at $z \sim 1$. We consider halos to be clusters if $M \geq 10^{14} h^{-1} M_{\odot}$ (i.e. 5971 or more particles); at $z = 0$ there are 909 clusters in the $\sigma_8 = 1.0$ box and 574 in the $\sigma_8 = 0.8$ box.

For the formation time studies, most of the definitions are straightforwardly derived from the cluster histories. We track the properties of all of the progenitor halos with more than 64 particles for all of our clusters. From these histories it is straightforward to find the mass of the largest progenitor as a function of time. To find mergers, the two largest predecessors are found for each cluster at an earlier time. The final cluster is said to have had a (major) merger between the earlier time and the later time if the ratio of particle numbers going from both of the predecessors into the final cluster is above some minimum⁸. In the case where the time interval of interest does not coincide with a dump time for the data, the two closest times bracketing the time of interest are taken, and the merger fraction is linearly interpolated between these (starting from the time closest to the time of interest). One relaxation time we consider is the crossing time, in this case we start at the earlier time and interpolate between final times.

We checked our definitions of mergers in two ways. Instead of using the mass of only progenitor particles which actually go into the final halo in the mass ratio, one can use the full mass of the progenitor halos, this changes the merged fraction by less than 5% for the longer time intervals and almost always less than 10% for the short time intervals. We prefer our definition as it might help counteract the inclusion of many unbound particles in halos due to our

⁸ This was in part to try to minimize the effect of particles which were not actually bound being taken to be part of a cluster’s predecessor.

FoF group finder. Secondly, we identify mergers by looking at the initial and final halos and comparing mass ratios of the initial halos, without tracking their intermediate behavior until they merged to the final halo. A concern was that two predecessors with an initial mass ratio of e.g. 1:5 might first become a mass ratio of 1:10, say, if the largest progenitor grew significantly in mass relative to the second largest, before merging. Looking at intermediate times, the mass ratio of predecessors is differs for the two definitions, but mostly for almost equal mass predecessors. Once the predecessor mass ratio drops to $\sim 1:3$ the scatter between the two ways of defining predecessor mass ratio gets quite small. Using the more accurate definition based on intermediate time steps produces a slightly larger number of recently merged clusters, again less than 5%. That is, our approximation in some cases underestimates the number of mergers by a small amount.

We vary the mass ratios and time intervals, and consider intervals equally spaced in real time, in light crossings (scaling as a) and in terms of “crossing times” (scaling as $(G\bar{\rho})^{-1/2} \sim a^{3/2}$). We call the lookback time the time at which the cluster is observed, and the relaxation time the interval prior to the lookback time within which the merger or mass jump (“large ΔM ”) has or hasn’t occurred. Intervals of 100, 300 and $600a h^{-1}\text{Mpc}$ light crossings correspond to approximately 1, 3 and $6 \times a/2$ Gyr. We call these $\delta\tau = 100, 300, 600 h^{-1}\text{Mpc}$ in the following. Although the simulations go back to $z \sim 2$, we only plot back to lookback times where the statistics have any constraining power.

We investigate three-body mergers as well, which we define as the case when the second and third largest predecessors each contribute to the final halo at least 20% of the mass contributed by the largest predecessor. Similarly, four-body mergers require the fourth largest predecessor to also contribute at least 20% of the mass contributed by the largest predecessor.

4 Results

4.1 Formation times and properties

A classic paradigm for cluster assembly histories is the spherical top-hat collapse model. In this model a uniform, overdense region “breaks away” from the expansion of the universe, evolving as a self-contained positive curvature universe. This toy model is often used to motivate the threshold density for virialization or to estimate formation times (49). The evolution of such perturbations does not closely resemble the rich structure seen in the formation of massive halos in N-body simulations, as noted by many authors referenced

above, however it is interesting to see how it performs nonetheless. We show in Fig. 1 the evolution of the peak circular velocity ($M \propto v_c^3$) of the most massive progenitor for 6 clusters, chosen at random from amongst the most massive ($M > 6 \times 10^{14} h^{-1} M_\odot$) in our $\sigma_8 = 0.8$ simulation. Since the mass in the spherical top-hat model is difficult to compare to simulations (it is constant and has uniform overdensity), we use peak circular velocity. The peak of the circular velocity curve, $v_c^2 \equiv GM(< r)/r$, is computed for each progenitor using the minimum of the cluster potential as a center for defining r . The dashed line shows the evolution predicted using the spherical top-hat collapse model for a cluster which virializes at the present. We see that the spherical infall description has a cluster growing most quickly right before virialization, while the clusters forming in a cosmological simulation have more of a steady growth over time. We have also marked on the plot four of the formation times defined and discussed below, z_{jump} , $z_{1/2}$, z_f and z_{tp} .

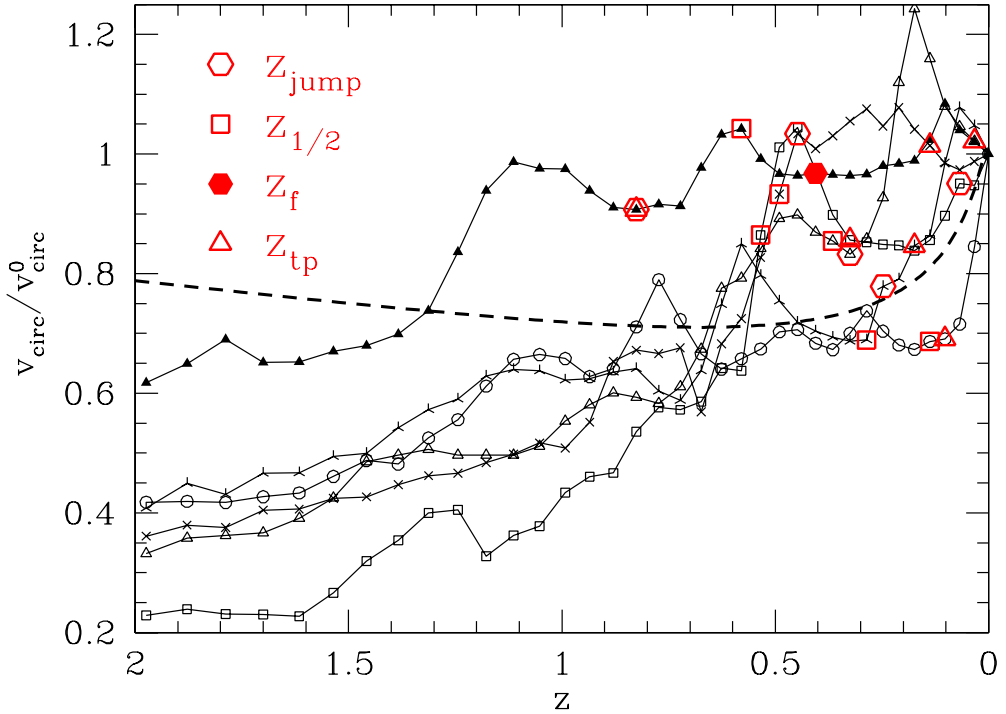


Fig. 1. The evolution of the peak circular velocity of the most massive progenitor for 6 massive clusters (symbols connected by solid lines) compared to spherical top-hat collapse of a cluster virializing at $z = 0$ (dashed). The cosmological model is our Λ CDM $\sigma_8 = 0.8$ model. The large symbols indicate various formation times discussed in the text, as indicated by the legend. Only the cluster denoted by the filled circle has a positive z_f .

A different view of the formation of clusters is given in Fig. 2 which focuses on

the same 6 clusters as Fig. 1. In the top panels we show the mass of the largest progenitor as a function of time. In the middle panel we show the ratio of the 1D velocity dispersion to the peak circular velocity – this has been used as a proxy for the degree of virialization of the clusters (50). In the lower panel we show the relation between the total kinetic and potential energy explicitly. Both energies have been computed using only the particles in the FoF group, but no proxy has been used, unlike the middle panel.

Even focusing only on the most massive progenitor, rather than the full merger tree, the upper panels show the rich phenomenology of cluster formation. There are several obvious mass jumps interspersed between periods of relatively smooth accretion. The lower panels show that the cluster is disturbed by mergers and large mass jumps with strong departures from the expected virial relation $2\text{KE} \simeq \text{PE}$. The departures last for several of our output times. The “standard” vacuum virial relation $2\text{KE} \equiv \text{PE}$ is not satisfied by these clusters even in their quiescent phase. The ratio $2\text{KE}/\text{PE}$ is typically larger than unity due to the steady accretion of material onto the cluster⁹ and there is an overall decline in $2\text{KE}/\text{PE}$ with time. Averaging over the entire cluster sample we find for objects of fixed mass the KE/PE ratio decreases with decreasing redshift. For objects at fixed redshift the ratio increases with increasing mass. For objects at fixed number density the ratio decreases with decreasing redshift. For fixed mass cut or number density the decline is steeper below $z = 1$ than above $z = 1$ and within errors the decline below $z = 1$ has the same shape for all samples. We can interpret this decline in KE/PE as due to the cessation of structure formation due to Λ domination below $z \sim 1$ (plus a small shift in the mass of objects currently undergoing rapid accretion). We will see a similar drop in merger activity below $z \sim 1$ in the next section.

We attempted to further quantify the relaxation of clusters to the background virial relation as a function of time since last major disturbance (c.f. Ref. (7)), but we found the scatter was too large for us to draw robust conclusions.

Even though cluster formation is a complex process it is sometimes useful to attempt to describe it with a single “formation time”. Any such compression of information must be imperfect, and to some extent arbitrary. Depending on the phenomenon of interest different times may be more or less appropriate. For this reason several definitions in the literature exist for the “formation time” of a cluster. We calculate several of these and their distributions for the $\sigma_8 = 0.8$ sample of 574 clusters below.

The first definition we consider is when a cluster had its most recent large ΔM , i.e. $M_f/M_i \geq 1.2$ in an interval $\delta\tau = 100 h^{-1}\text{Mpc}$. In this section a mass “jump” refers to a mass gain of at least this much. For any cluster z_{jump} is the

⁹ This can be thought of as a surface pressure term which modifies the virial relation, boosting the kinetic energy.

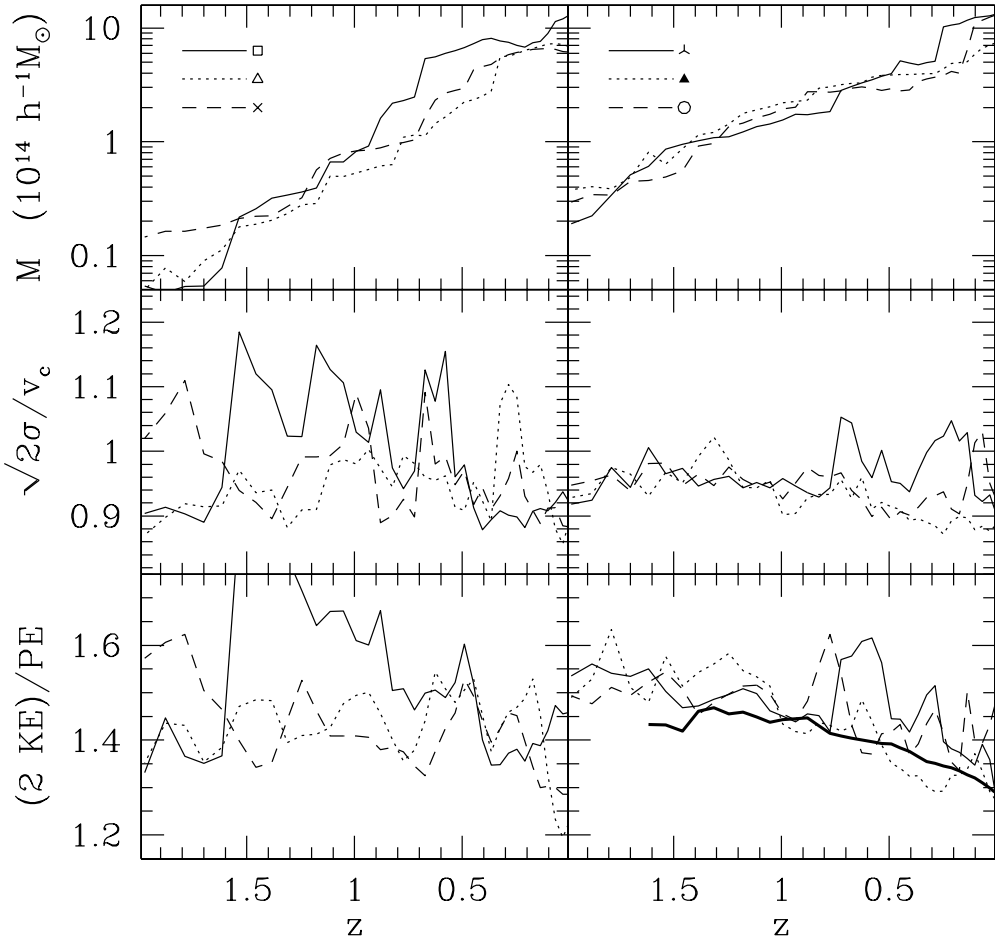


Fig. 2. A view of cluster formation for the same 6 massive clusters as in Fig. 1 (see inset legend for correspondence). The left and right columns show 3 clusters each. The top panel shows the mass accretion history since $z = 2$, the middle panel shows the ratio of velocity dispersion to circular velocity (which has been used previously as a proxy for degree of virialization) while the lower panels show the virial ratio, $2\text{KE}/\text{PE}$, as a function of time (see text). In the lower right panel, the heavy solid line is the virial ratio averaged over all clusters with $M > 10^{14} h^{-1} M_\odot$ at the given redshift. The first point, $z \simeq 1.6$, has 3 clusters above the threshold.

redshift of the most recent such jump. In our sample 13 clusters had no large mass jumps at any time after $z \sim 2$, two of these clusters are more massive than $3 \times 10^{14} h^{-1} M_\odot$. Ref. (7) found that 2 out of their sample of 20 did not have any large mass jumps. Another common definition is when the cluster has reached at least half its mass, for this time there is an analytic formula (51) which was tested in (and improved using) simulations in Ref. (52). We define $z_{1/2}$ as the earliest output time when the cluster had at least half of its mass. The relation between these two definitions is shown in the upper

left hand panel of Fig. 3. There is a large amount of scatter between the two definitions but there is a striking transition at $z = 0.5$. For clusters which have not reached half of their present day mass before $z = 0.5$, almost all have had a large ΔM jump after reaching half-mass, i.e. they have at least half of their mass before they have their last large mass jump. However, for clusters which attained $z_{1/2}$ before redshift $z = 0.5$ (286 clusters), slightly under one third (80) had their most recent mass jump even earlier (i.e. $z_{\text{jump}} > z_{1/2}$). An intuitive reason for this is that clusters which reached half of their mass early on have not been gaining mass quickly and so are less likely to have large mass jumps after $z_{1/2}$. This general shape persists if one considers some other “formation time” such as $z_{1/3}$ or $z_{3/4}$ (with obvious definitions), the z value where z_{jump} starts becoming larger (that is, earlier) than $z_{1/3}(z_{3/4})$ is larger (smaller) than that for $z_{1/2}$. A larger fraction (12/33) of the clusters with mass greater than $3 \times 10^{14} h^{-1} M_{\odot}$ and $z_{1/2} > 0.5$ had $z_{\text{jump}} > z_{1/2}$. If one is interested in formation times in order to find undisturbed clusters, for lower redshifts it appears that z_{jump} may be a more conservative estimate.

A third definition of a cluster formation time is when the potential well of the object becomes deep enough to be considered “a cluster”. We take this, somewhat arbitrarily, to be when the object has reached $10^{14} h^{-1} M_{\odot}$, and call this z_{14} .

All of these definitions rely on special events in the mass accretion history. An alternative is to use the whole history of the most massive progenitor. While this is less information than in the entire tree, it provides a global view of the formation process. For galaxy sized halos, Ref. (10) found that the mass accretion histories could be fit by $M(a) = M_0 e^{-2a_f z} = M_0 e^{-2z/(1+z_f)}$, and that z_f correlated well with other cluster properties, i.e. concentration. Ref. (8) found that for clusters they could obtain better fits if they generalized the function to $\tilde{M}(a) = M_0 a^p e^{-2\tilde{a}_f z} = a^p M(a)$, where $\tilde{a}_f = 1/(1+\tilde{z}_f)$. A different fit to the mass accretion history, and a different formation time, was proposed by Ref. (6). These authors found that halos generally transition from a period of rapid accretion to a phase of slow accretion and used the transition redshift, z_{tp} as a proxy for “formation” time.

We fit these three parameterizations to our sample. Although these parameterizations do describe general trends in the cluster mass histories, good fits were not found for all the cluster histories. We estimate z_f through a least squares fit of $\ln(M_i/M_0)$ against z_i , with all points being equally weighted. With $p = 0$ we find poor fits for several clusters, making the results sensitive to the z -range used and the interpretation of the fit coefficient difficult. The generalized form of Ref. (8) still does not produce good fits for many of the clusters, and in addition many of the best fits have minima in the accretion histories which we regard as unphysical. We investigated the dependence on the range of z used in the fit. Ref. (8) fit their z_f to histories for $0 \leq z < 0.5$

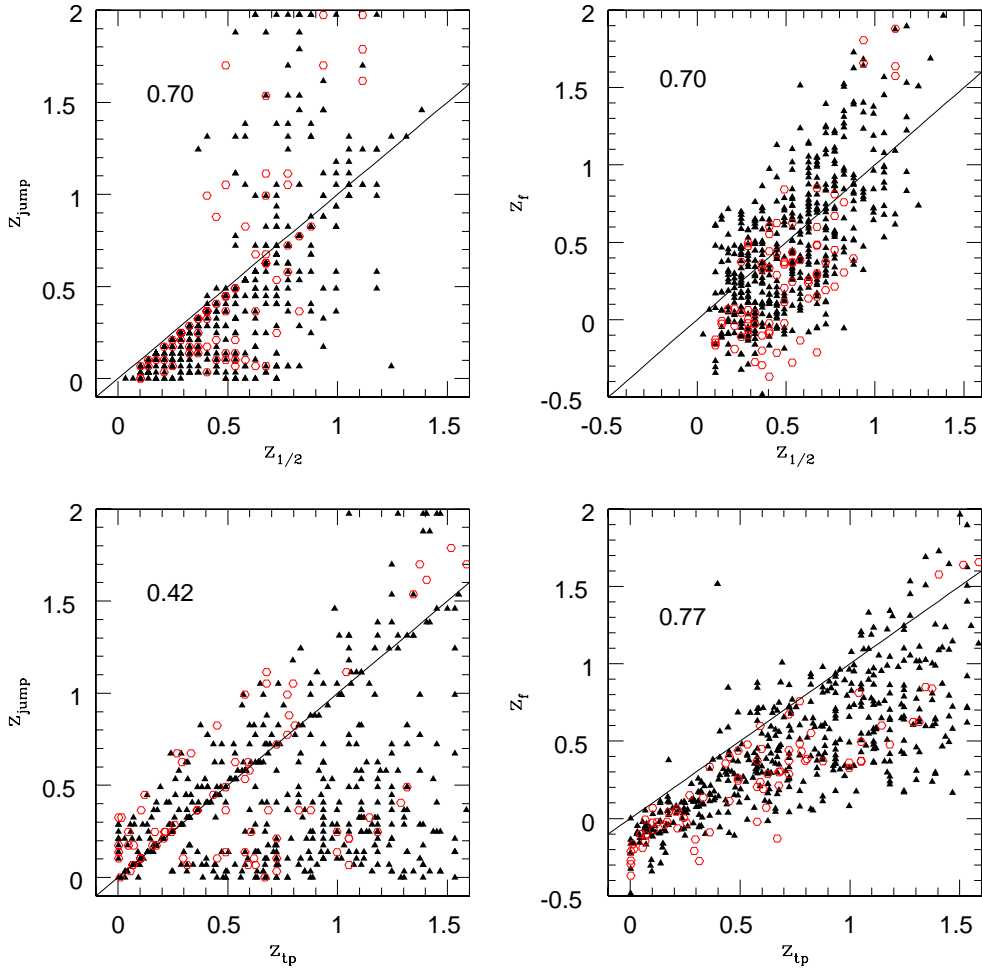


Fig. 3. Top left: $z_{1/2}$ vs. z_{jump} . The 13 clusters with no large ΔM in the simulations are not shown as they have $z_{\text{jump}} > 2$. Top right: $z_{1/2}$ vs. z_f . Lower left: z_{tp} vs. z_{jump} . Lower right: z_{tp} vs. z_f . The red circles correspond to clusters with $M > 3 \times 10^{14} h^{-1} M_{\odot}$. The correlation coefficient, r , for each case is shown at upper left.

and for $0 \leq z < 10$ and found that the results were consistent. We found extremely large variations comparing $0 \leq z < 0.5$ and $0 \leq z < 2.07$. Even some clusters which gained more than 90% of their mass in the range we consider have z_f which depends sensitively on the fit range. This is a simple consequence of the fact that the functional form does not well describe the shapes of the mass accretion histories of these objects. Finally we note that for clusters with recent mass jumps the fit prefers $z_f < 0$. As it is very plausible to say that these systems are still in the process of forming we report these values below without renormalization. We compare this formation time z_f with $z_{1/2}$ at upper right in Fig. 3; they are correlated (as also found by Ref. (8)).

We also use a least-squares fit to find the z_{tp} of Ref. (6). Here the mass accretion history is fit to the form $M_i/M_{\text{tp}} = f(\rho_{\text{vir}}(z_{\text{tp}})/\rho_{\text{vir}}(z_i))$ where $\rho_{\text{vir}}(z)$ is the virial density at redshift z computed from spherical top-hat collapse and f is a specified functional form (6). We quote the value of z_{tp} in the range $0 < z < 2$ which best fits¹⁰ f . We show in Fig. 3, bottom, the comparison of this “turning point” time z_{tp} with z_{jump} and z_f above. The largest correlation is between z_{tp} and z_f , as shown in Fig. 3.

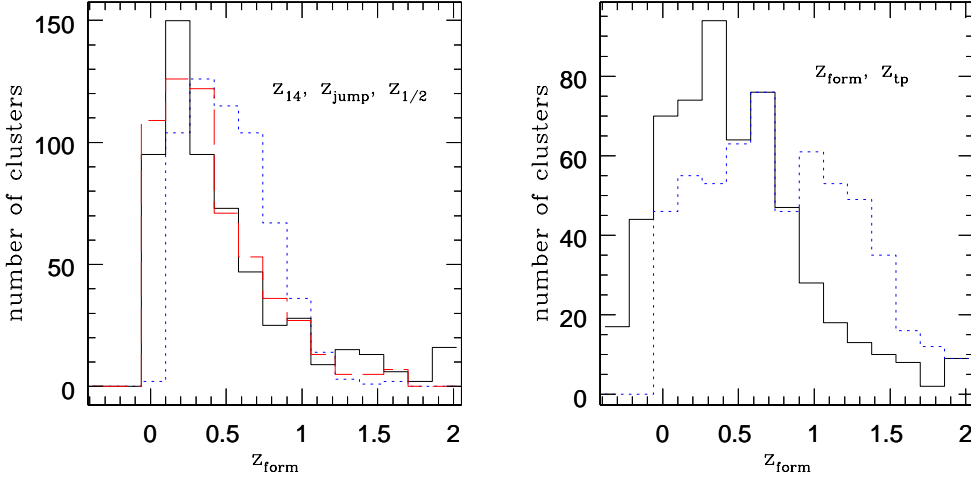


Fig. 4. Distributions of different formation time definitions for all clusters in the $\sigma_8 = 0.8$ sample. On left are the distributions for z_{jump} (solid line), $z_{1/2}$ (dotted line) and z_{14} (dashed line). At right, is the distribution for z_f (solid line) and z_{tp} (dotted line). Note that some clusters have $z_f < 0$. See text for further definitions of these formation times.

In addition to comparing the different formation times to each other, we also use the cluster sample to get a snapshot of the formation time distribution. In Fig. 4 we show the distributions of these different formation times for all the clusters at $z = 0$. Clusters which had no large mass jump since $z = 2$ are put in the $z_{\text{jump}} = 2$ bin for completeness.

There is quite a spread in these formation times, however some trends are clear. By $z = 0.2$ over 85% of the clusters have had their last large mass jump and over 81% of them have formed according to the definition of Ref. (10), while 88% of them have at least half of their mass. The different definitions have different biases though, e.g., only the definition of Ref. (10) can go negative.

Part of our difficulty in fitting smooth curves to the mass accretion histories is the presence of significant mass jumps. The statistics of these jumps are

¹⁰ In fact we fit M not M_{vir} but this should have little effect since $M_{\text{vir}} \simeq 1.08 M$ at $z = 0$ and $\simeq 1.05 M$ at high z .

themselves of interest. Fig. 5 gives the distribution of the number of times since $z = 2$ that the mass of each cluster changes by 20%. This is the same quantity considered by Ref. (7) for their sample of 20 clusters more massive than $1.2 \times 10^{14} h^{-1} M_\odot$ – our sample is more than an order of magnitude larger allowing us to more completely characterize the distribution. We find that there is little dependence on the cluster mass – lines for clusters above 1, 2 and $3 \times 10^{14} h^{-1} M_\odot$ are shown. The average (median) number of jumps for each of these samples is 4.0 (4), 4.3 (4), 4.6 (5), respectively, with a wide spread. The right panel of Fig. 5 shows how much of the cluster mass is gained in these events – slightly less than half of the clusters (272/574) get at least half of their mass in jumps of 20% or larger. For the $M > 3 \times 10^{14} h^{-1} M_\odot$ subsample the fraction is larger: 41/79.

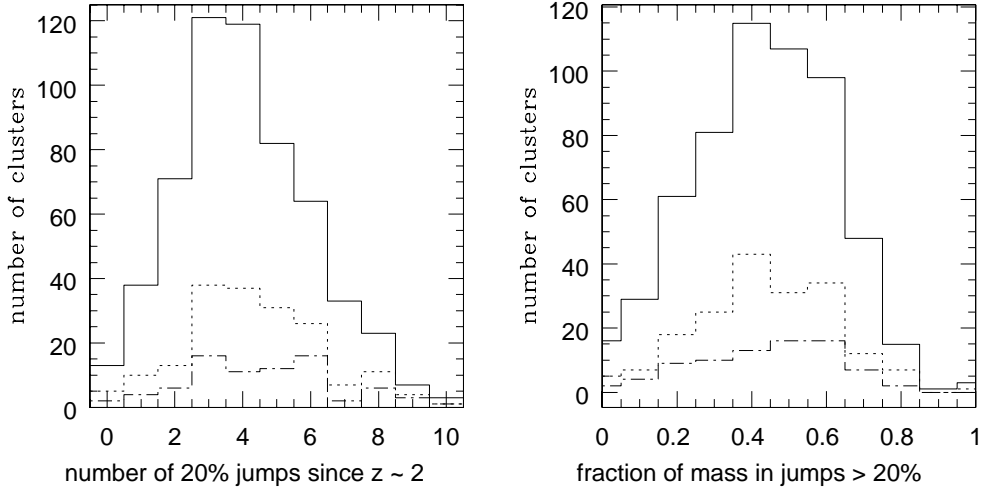


Fig. 5. Left: Number of clusters with N mass jumps $M_f/M_i \geq 1.2$ since $z = 2$. The three lines are for clusters with $M > 1$, 2, and $3 \times 10^{14} h^{-1} M_\odot$. The average number (median number) of jumps are 4.0(4), 4.3(4), 4.6(5) respectively. Right: number of clusters with a given fraction of the total cluster mass obtained in mass jumps $M_f/M_i \geq 1.2$.

4.2 Time dependence of recently merged or large ΔM cluster fraction

The above shows that the present day cluster population has a very wide spread of formation times and frequent major disruptions. For observational purposes, another question is: how many clusters at a given redshift (“lookback time”) have had a large disruption recently (within a given “relaxation time”).

The fraction of clusters with a large mass change ΔM in a given interval is shown in Fig. 6, top, as the dotted lines. This is the total mass change, via mergers *or* accretion, within the 1.0 and 2.5 Gyr time intervals. The two lines

show the fraction of clusters with final/initial mass ≥ 1.2 and 1.33 (these ratios were chosen by Refs. (7) and (5)), with the lower line for the higher mass ratio.

We may be interested in the most disruptive mass gains, which occur when the progenitor ratios are smallest. We refer to these events as major mergers. Figure 6, top, also shows the fraction of recently merged clusters as a function of time for minimum mass ratios 1:3, 1:5 and 1:10. For a lookback time of 7 Gyr ($z \sim 0.8$) for instance and the 2.5 Gyr relaxation time, this means considering predecessors 9.5 Gyr ago (at $z \sim 1.6$).

The error bars are calculated using binomial statistics. If M of the N clusters have merged the most likely¹¹ fraction is $f = M/N$ with variance:

$$\sigma_f^2 = \frac{M(N - M) + 1 + N}{(N + 2)^2(N + 3)}. \quad (1)$$

We use symmetric error bars. One can see here that the number of clusters which have had a recent major merger increases in the past, reaching a dramatic 80% for 1:10 or smaller mergers 7 Gyr ago (around $z \sim 0.83$) for a relaxation time of 2.5 Gyr. For shorter relaxation times fewer mergers have occurred, as expected. For fixed relaxation times the amount of accretion relative to merging changes with lookback time.

In the lower two panels different relaxation times are considered. For some phenomena associated with mergers the relaxation times of interest depend on the time of observation. We saw in the previous section that departures from the virial relation lasted several hundred Mpc of conformal time. This is not unexpected. A typical relaxation time is likely some fraction of the halo dynamical time. Since clusters have $\bar{\rho} \sim 10^2 \rho_{\text{crit}}$ and characteristic times scale as $\rho^{-1/2}$, typical timescales should be $0.1 t_{\text{H}}$ where $t_{\text{H}} \equiv H^{-1}$ is the Hubble time. Ref. (7) noted that X-ray disturbances in their gas simulations lasted $\delta\tau = 300 h^{-1} \text{Mpc}$ (scaling as a rather than the crossing time $\sim a^{3/2}$). This corresponds to roughly $1.3 h^{-1} \text{Gyr}$ at the present, and shorter times in the past. Simulations reported in (21) have major merger related disturbances lasting approximately one crossing time. From (53), we take this to be 1 Gyr at the present. These two relaxation times are used in Fig. 6 bottom, with that found by Ref. (7) at left and $a^{3/2}$ Gyr at right. For the latter case, the a used is for the initial time, before the merger, as clusters which merge later have a larger a and thus longer relaxation time, and thus will also still be unrelaxed at the given lookback time. The ratio between the fractions with mergers and large ΔM does not change as much with lookback time compared to the case where the relaxation time was independent of the lookback time. This suggests that equating large ΔM jumps with mergers is more reliable for

¹¹ The mean value is $(M + 1)/(N + 2)$.

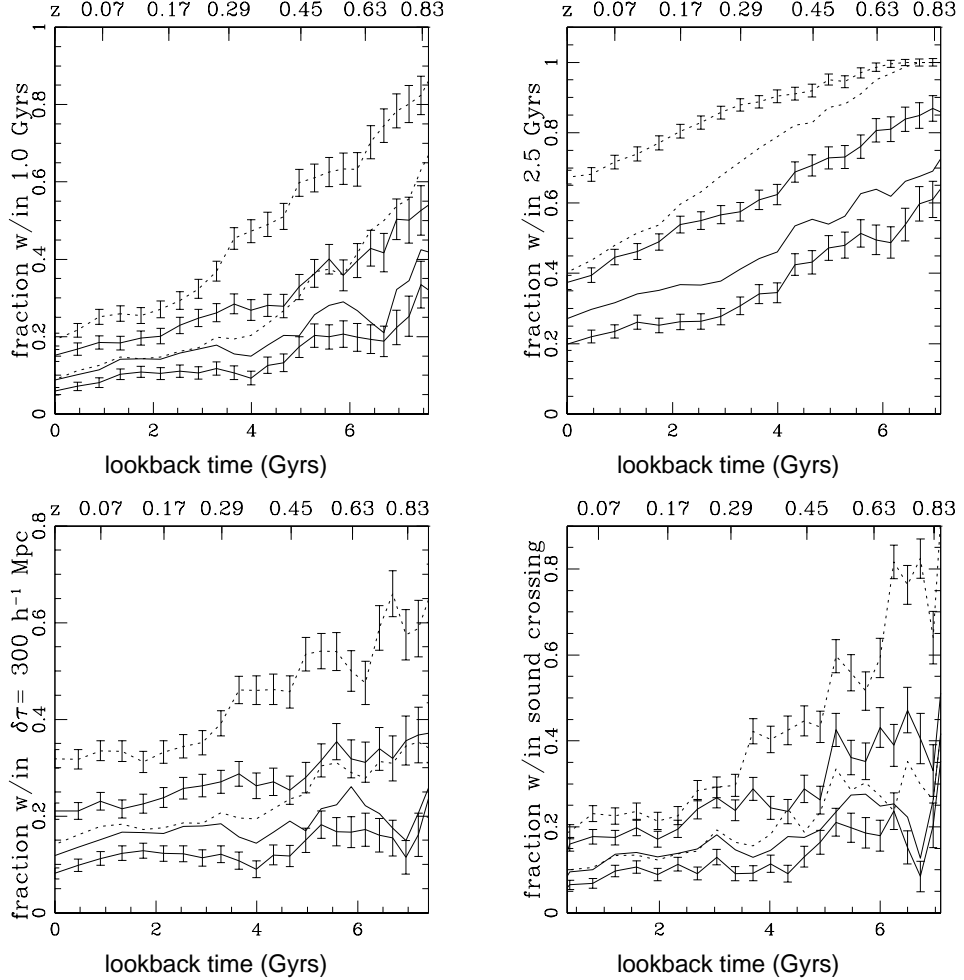


Fig. 6. Top: Merger fractions in the previous 1.0 Gyr, 2.5 Gyr, $\delta\tau = 300 h^{-1} \text{Mpc}$ and t_{cross} , as a function of lookback time to clusters, for $\sigma_8 = 0.8$. The solid lines give the fraction of clusters ($M \geq 10^{14} h^{-1} M_\odot$) whose two largest predecessors contribute numbers of particles with ratios of 10:1 or smaller, 5:1 or smaller and 3:1 or smaller (top to bottom) at given lookback times. The dotted lines are the fraction of clusters which have $M_f/M_i \geq 1.2$ and 1.33. For clarity (binomial) error bars are shown for only some of the lines. The others are similar.

phenomena whose relaxation times scale with a .

In Fig. 7 we compare different samples of clusters, changing cosmology ($\sigma_8 \rightarrow 1.0$) and mass (taking $M > 3.0 \times 10^{14} h^{-1} M_\odot$). At the top are the fractions of recently merged or recent large ΔM clusters for both $\sigma_8 = 0.8$ and $\sigma_8 = 1.0$, for the relaxation time is $\delta\tau = 600 h^{-1} \text{Mpc}$. At present this lookback time is slightly over 2.5 Gyr. The error bars are smaller for $\sigma_8 = 1.0$ because there are nearly twice as many clusters in the sample. The $\sigma_8 = 1.0$ clusters have had fewer mergers and mass jumps than those for $\sigma_8 = 0.8$; clustering is less

evolved for $\sigma_8 = 0.8$ so a cluster at fixed mass is more likely to be forming in our redshift range. At the bottom, the recently merged or recent large ΔM clusters are shown for more massive clusters, $M > 3.0 \times 10^{14} h^{-1} M_\odot$, with $\sigma_8 = 0.8$, for relaxation times of $\delta\tau = 300 h^{-1} \text{Mpc}$ (left) and for 2.5 Gyr (right). As there are significantly fewer clusters (79 rather than 574) at $z = 0$, the error bars are a lot larger and are only shown for the top line. Comparing with the same plots in Fig. 6, it is seen that more of the massive clusters have had recent major mergers.

Values for $\sigma_8 = 1$ are reported in Tables 1-4 for four lookback times, along with N_{clus} so that the errors can be estimated.

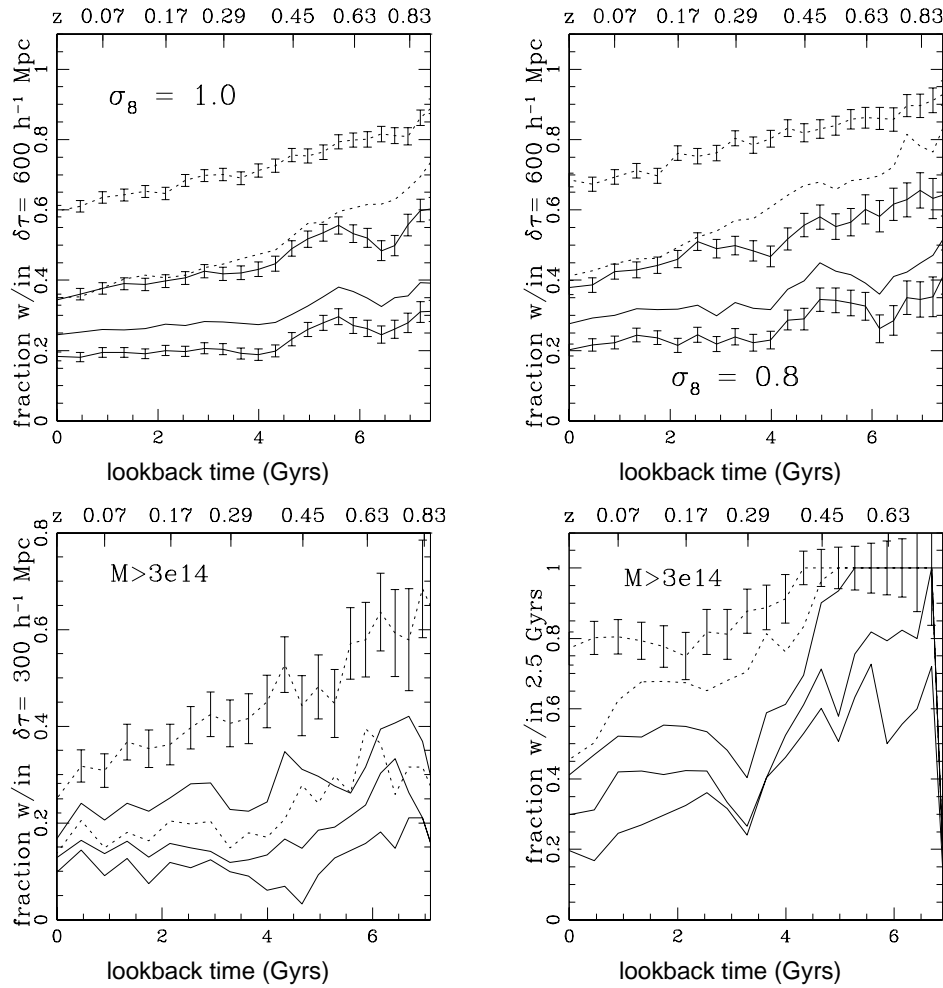


Fig. 7. Top: recent mergers or large ΔM for a relaxation time of $\delta\tau = 600 h^{-1} \text{Mpc}$, for two values of σ_8 . Bottom: the recently merged/large ΔM fraction for clusters with $M > 3.0 \times 10^{14} h^{-1} M_\odot$, for relaxation times of $\delta\tau = 300 h^{-1} \text{Mpc}$ and 2.5 Gyr. Smooth lines are 1:10, 1:5 and 1:3 predecessor mass ratios, dotted lines are $M_f/M_i \geq 1.2, 1.33$ (top to bottom). Errors as before.

lookback time	1:3	1:5	1:10	20%	25%	N_{clus}
0.0	0.07	0.08	0.12	0.14	0.08	909
2.2	0.08	0.11	0.18	0.23	0.13	739
4.0	0.09	0.13	0.22	0.34	0.15	573
6.2	0.19	0.26	0.39	0.60	0.35	346

Table 1

The number of mergers or large ΔM events within the previous 1 Gyr as a function of lookback time for our $\sigma_8 = 1.0$ simulation, comparable to Fig. 6 upper left for $\sigma_8 = 0.8$.

lookback time	1:3	1:5	1:10	20%	25%	N_{clus}
0.0	0.18	0.24	0.34	0.59	0.34	909
2.2	0.22	0.31	0.45	0.73	0.49	739
4.0	0.29	0.38	0.57	0.83	0.67	573
6.2	0.45	0.54	0.72	0.97	0.90	346

Table 2

The number of mergers or large ΔM events within the previous 2.5 Gyr as a function of lookback time for our $\sigma_8 = 1.0$ simulation, comparable to Fig. 6 upper right for $\sigma_8 = 0.8$.

lookback time	1:3	1:5	1:10	20%	25%	N_{clus}
0.0	0.08	0.11	0.16	0.23	0.12	909
2.2	0.10	0.13	0.21	0.28	0.16	739
4.0	0.09	0.12	0.21	0.33	0.15	573
6.2	0.16	0.22	0.32	0.48	0.26	346

Table 3

The number of mergers or large ΔM events within the previous $\delta\tau = 300 h^{-1} \text{Mpc}$ as a function of lookback time for our $\sigma_8 = 1.0$ simulation, comparable to Fig. 6 lower left for $\sigma_8 = 0.8$.

lookback time	1:3	1:5	1:10	20%	25%	N_{clus}
0.4	0.06	0.08	0.12	0.13	0.09	872
2.3	0.08	0.11	0.19	0.21	0.12	718
4.3	0.10	0.13	0.23	0.33	0.15	516
6.3	0.14	0.18	0.33	0.57	0.26	291

Table 4

The number of mergers or large ΔM events within the previous $a^{3/2}$ Gyr as a function of lookback time for our $\sigma_8 = 1.0$ simulation, comparable to Fig. 6 lower right for $\sigma_8 = 0.8$.

For all relaxation times there is an increase in the fraction of recently merged or recent large ΔM as the lookback time increases, i.e. there were more major mergers and large mass jumps in the past. The fraction depends on the relaxation time chosen. An overview is provided in Fig. 8 where we compare the ratios of merged and large ΔM samples near the present to that of about 6 Gyr ago, for several different relaxation times in our two simulations. A doubling of the recently merged or recent large ΔM fraction between the present and $z \sim 0.67$ is not uncommon, and sometimes even larger increases occur. The errors in these ratios for the relaxation time of $\delta\tau = 100 h^{-1}\text{Mpc}$ are quite large. For $\sigma_8 = 0.8(1.0)$, from 44(29)% for the 1:3 mergers to 32(28)% for $M_f/M_i \geq 1.2$. For the other relaxation times the errors on the ratio are the largest for the 1:3 mergers (10-25%) and smallest for the mass jumps with $M_f/M_i \geq 1.2$ (3-12%). The errors on the other cases fall in between. More details can be obtained from the earlier plots and the Tables.

Another question of interest might be: in how many major mergers do three or four predecessors have comparable mass? We took one particular definition as described in the methods section. These three-body mergers were fairly common, the exact numbers depend upon relaxation times considered. For the $\sigma_8 = 0.8$ case, about 15% of the 1:5 mergers were three-body for $\delta\tau = 30 h^{-1}\text{Mpc}$ and slightly less than 30% for $\delta\tau = 600 h^{-1}\text{Mpc}$ on average, with little evidence of growth with time. For $\sigma_8 = 1.0$ the fraction of three-body mergers to 1:5 major mergers was closer to 10% on average and seemed to grow with time for $\delta\tau = 300 h^{-1}\text{Mpc}$. For $\delta\tau = 600 h^{-1}\text{Mpc}$ this growth was more evident, starting around 12% and growing to around 30%. For fixed relaxation times, 2.5 (1.0) Gyr, the fraction of three-body major mergers to 1:5 major mergers showed a definite increase with lookback time. For $\sigma_8 = 0.8$ it started at 30% (10%) and grew to 80% (35%) at lookback times of 7 Gyr. For $\sigma_8 = 1.0$ the fraction started at 12% (5%) and grew to 55% (25%) at lookback times of 7 Gyr. This means that even though a 1:5 merger might not be considered “major” by some definitions, it is very possible that there are two of these going on at the same time, making these mergers more energetic.

There were many fewer four-body mergers. The largest effect was for the 2.5 Gyr relaxation time, where four-body mergers were about one third of the three-body mergers. In the largest case, for $\sigma_8 = 0.8$ and 2.5 Gyr relaxation time, the total fraction of clusters which had had a recent four-body merger only reached 5% or above for lookback times greater than 4 Gyr.

5 Conclusions

Clusters of galaxies represent the current endpoint of structure formation. As the largest systems which have had time to virialize in a universe with hier-

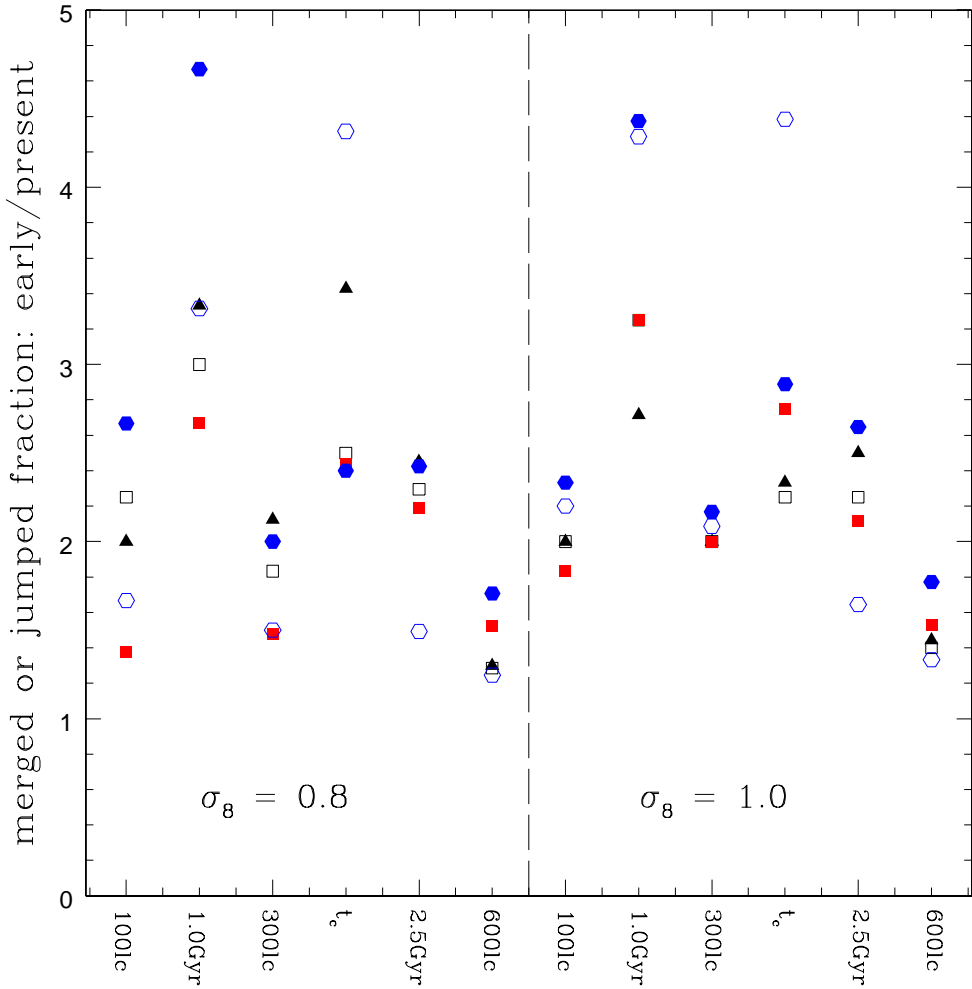


Fig. 8. Summary of change in recent merger/recent large ΔM fraction of clusters with time: (fraction 6.2 Gyr ago)/(fraction at present) for most, (fraction 6.3 Gyr ago)/(fraction 0.4 Gyr ago) for the $a^{3/2}$ relaxation time case. The various relaxation times are listed at the bottom: 100t, 300t, 600t ($\delta\tau = 100, 300, 600 h^{-1} \text{Mpc}$ respectively), $t_{\text{cross}} = a^{3/2} \text{Gyr}$, and 1.0 and 2.5 Gyr. Filled triangles are 1:3 mergers, open squares are 1:5 mergers, filled squares are 1:10 mergers, open circles are 20% mass jumps, filled circles are 33% mass jumps. The errors are fairly large at the early time but one can see that a doubling of the recently merged or large ΔM fraction between the present and $z \sim 0.8$ is not uncommon and sometimes even larger increases occur.

archical structure formation, they make excellent laboratories for cosmology, large-scale structure and galaxy formation. The formation of galaxy clusters via a combination of mergers and accretion of smaller objects is crucial to understanding many of their present day properties.

In this paper we investigated the formation of galaxy clusters in some detail, and the major events which define this process, extending earlier studies (2; 3;

4; 5; 6; 7; 8; 9; 12) discussed in §2. While galaxy cluster formation properties can be reliably calculated with the present generation of large, high-resolution N-body simulations, it is difficult to find specific numbers in the literature. To remedy this we have calculated, for a sample of hundreds of clusters, the degree of virialization, formation time, and for two values of the clustering amplitude σ_8 , the fraction of disturbed galaxy clusters for many definitions of disturbed.

We began by showing the time histories of a few clusters to illustrate the typical formation pattern: periods of smooth accretion punctuated by large increases in mass. We then turned to various characterizations of this process, applied to our statistical sample as a whole.

We first calculated the ratio of kinetic to potential energy. At early times clusters are hotter than the vacuum virial relation (2KE=PE) would predict due to continuous infall of material. With the onset of Λ domination and the cessation of structure growth the excess kinetic energy drops and their mass accretion rate slows.

We then turned to formation time definitions in the literature; while no single number can capture the complexity of a cluster merging tree, the concept of a formation time encodes much useful information. We compared different formation time definitions which are relevant for different types of observations. For instance a recent large mass jump may not be of interest if one only wants to know when the cluster first was detectable by SZ decrement (which presumably depends more on the depth of the potential well), but may be relevant for studies which rely on a cluster being old enough to be dynamically relaxed. The different formation times we considered are correlated, with large scatter. Formation times relying upon a smooth parameterized fit to galaxy cluster histories were most correlated with each other, but the results were sensitive to the fit methodology, due to the large amount of recent sporadic mass gain. We compared the distributions of the different formation times for our whole cluster sample and for our more massive clusters, again finding some correlation but also significant scatter.

We then turned from smooth parameterizations to the characteristic abrupt jumps in mass over time for galaxy clusters. On average, galaxy clusters have had at least 4 large mass jumps since $z \sim 2$, this number increases with cluster mass; about half of the clusters get at least half of their mass in these jump events.

The above measurements were for our $\sigma_8 = 0.8$ sample of 574 clusters. The second part of the paper reported the time dependence of the fraction of clusters which have had a recent mass jump or major merger, using in addition a $\sigma_8 = 1.0$ sample of 909 clusters. These fractions should be of use for estimates

of the number of “relaxed” clusters available in surveys (given a relaxation time for the phenomena of interest) and for helping to constrain relaxation times for phenomena associated with mergers or mass jumps where the phenomenon’s occurrence fraction has been measured but not its relaxation time. In Figs. 6-8 and tables 1-4 we give the merger fractions for a number of different situations. These fractions also serve to quantify the previously seen trend of more recent mergers (fractionally) at higher redshift. Comparing $z = 0$ with $z = 0.67$ (about 6 Gyr ago), the fraction of clusters which had a recent merger or mass jump is doubled by almost any definition and for some definitions the increase is even larger.

JDC thanks T. Abel, S. Allen, G. Bryan, J. Hennawi, R. Kneissl, A. Kravtsov and P. Ricker for helpful discussions and was supported in part by NSF-AST-0205935. MJW was supported in part by NASA and the NSF.

References

- [1] C.A. Metzler, M. White, M. Norman, C. Loken, *ApJ* 520 (1999) L9.
C.A. Metzler, M. White, C. Loken, *ApJ* 547 (2001) 560.
D. Clowe, G.A. Luppino, N. Kaiser, I.M. Gioia, *ApJ* 539 (2000) 540.
H. Hoekstra, *MNRAS* 339 (2003) 1155.
N. Padmanabhan, U. Seljak, U.-L. Pen, *New Astron.* 8 (2003) 581.
J.F. Hennawi, D.N. Spergel, *ApJ* 624 (2005) 59.
R. de Putter, M. White, *New Astron.*, in press [astro-ph/0412497].
J. Hennawi, N. Dalal, P. Bode, J. Ostriker, [astro-ph/0506171].
- [2] G. Tormen, F.R. Bouchet, S.D.M. White, *MNRAS* 286 (1997), 865.
- [3] G. Tormen, *MNRAS* 297 (1998), 648.
- [4] J.M. Colberg, S.D.M. White, A. Jenkins, F. R. Pearce, *MNRAS* 308 (1999), 593.
- [5] S. Gottlöber, A. Klypin, A.V. Kravtsov, *ApJ* 546 (2001) 223.
- [6] D.H. Zhao, Y.P. Jing, H.J. Mo, G. Boerner, *ApJ* 597L (2003) 9.
- [7] D.R. Rowley, P.A. Thomas, S.T. Kay, *MNRAS* 352 (2004) 508.
- [8] A. Tasitsiomi, A.V. Kravtsov, S. Gottlöber, A.A. Klypin, *ApJ* 607 (2004) 125.
- [9] M.T. Busha, F.C. Adams, R.H. Wechsler, A.E. Evrard, *ApJ* 596 (2003) 713.
- [10] R.H. Wechsler, et al, *ApJ* 568 (2002) 52.
- [11] F. van den Bosch, *MNRAS* 331 (2002), 98
- [12] J.R. Bond, S. Cole, G. Efstathiou, N. Kaiser, *ApJ* 379 (1991) 440.
D. Richstone, A. Loeb, E.L. Turner, *ApJ* 393 (1992) 477.
C.G. Lacey, S. Cole, *MNRAS* 262 (1993) 627.
C.G. Lacey, S. Cole, *MNRAS* 271 (1994) 676.
T. Kitayama, Y. Suto, *MNRAS* 280 (1996) 638.
T. Kitayama, Y. Suto, *ApJ* 469 (1996) 480.

W.J. Percival, L. Miller, MNRAS 309 (1999) 823.
 W.J. Percival, L. Miller, J.A. Peacock, MNRAS (2000) 318, 273.
 R. Somerville, et al., MNRAS 316 (2000) 479.

[13] J.D. Cohn, J.S. Bagla, M. White, MNRAS 325 (2001) 1053.
 [14] R.C. Nichol, ASPC 268 (2002) 57.
 [15] R.A. Sunyaev, Ya. B. Zel'dovich, Comm. Astrophys, Space Phys., 4 (1972) 173.
 R.A. Sunyaev, Ya. B. Zel'dovich, ARA&A, 18 (1980) 537.

[16] M. White, L. Hernquist, V. Springel, ApJ 579 (2002) 16.

[17] P.M. Motl, E.J. Hallman, J.O. Burns, M.L. Norman, preprint [astro-ph/0502226].

[18] P. Koch, in “The Future of Cosmology with Galaxy Clusters” (Kona, Hawaii, 2005).

[19] C.L. Sarazin 2005, in “The Future of Cosmology with Galaxy Clusters” (Kona, Hawaii, 2005).

[20] S. Schindler, E. Muller, A&A 272 (1993) 137.
 K. Roettiger, J.O. Burns, C. Loken, ApJ 473 (1996) 651.
 M. Takizawa, ApJ 520 (1999) 514.
 P. Blasi, APh 15 (2001) 223.
 B.F. Mathiesen, A.E. Evrard, ApJ 546 (2001) 100.
 O. Muanwong, P.A. Thomas, S.T. Kay, F.R. Pearce, MNRAS 336 (2002) 527.
 E. Torri, et al., MNRAS 349 (2004) 476.

D.R.. Wik, C.L. Sarazin, P.M. Randall, P.M. Ricker, 2005, to appear (reported at Kona meeting on the Future of Cosmology with Galaxy Clusters).

[21] P.M. Ricker, C.L. Sarazin, ApJ 561 (2001) 621.
 [22] S.W. Randall, C.L. Sarazin, P.M. Ricker, ApJ 577 (2002) 579.

[23] R. Somerville, T. Kolatt, MNRAS 305 (1999) 1.

[24] D.A. Buote, in Merging Processes in Clusters of Galaxies, eds., L. Feretti, I.M.Gioia, G. Giovannini, ASSL. 272 (2002) 79 [astro-ph/0106057].

[25] C. Jones, W. Forman, ApJ 511 (1999) 65.

[26] J.J. Mohr, A.E. Evrard, D.G. Fabricant, M.J. Geller, ApJ 447 (1995) 8.

[27] P.L. Gomez, et al., ApJ 474 (1997) 580.
 E. Rizza, et al., MNRAS 301 (1997) 328.
 M. Bliton, et al., MNRAS 301 (1998) 609.
 P.L. Gomez, J.P. Hughes, M. Birkinshaw, ApJ 540 (2000) 726.
 B. Kolokotronis, S. Basilakos, M. Plionis, I. Georgantopoulos, MNRAS 320 (2001) 49.

[28] P. Schuecker, H. Boehringer, T.H. Reiprich, L. Feretti, A&A 378 (2001) 408.

[29] W.S. Burgett, MNRAS 352 (2004) 605.

[30] J.C. Tsai, D.A. Buote, MNRAS 282 (1996) 77.

[31] T. Jeltema, C.R. Canizares, M.W. Bautz, D.A. Buote, ApJ, in press [astro-ph/0501360].

- [32] P.A. Thomas, et al., MNRAS 296 (1998), 1061
T. Suwa, A. Habe, K. Yoshikawa, T. Okamoto, ApJ 588 (2003) 7
- [33] L. Feretti, preprint [astro-ph/0406090].
- [34] C.L. Sarazin, preprint [astro-ph/0406181].
- [35] G. Giovannini, L. Feretti, in *Merging Processes of Galaxy Clusters*, eds., L. Feretti, I.M. Gioia & G. Giovannini, ASSL 272 (2002) 197.
- [36] A.C. Fabian, S.J. Daines, MNRAS 252 (1991) 17.
A.C. Edge, G.C. Stewart, A.C. Fabian, MNRAS 258 (1992) 177.
S.W. Allen, MNRAS 296 (1998) 392
P. Ricker, Talk at Aspen meeting on Galaxy Clusters (Aspen, 1998).
- [37] F.E. Bauer, A.C. Fabian, J.S. Sanders, S.W. Allen, R.M. Johnstone, R.M., preprint [astro-ph/0503232].
- [38] P.M. Motl, J.O. Burns, C. Loken, M.L. Norman, G. Bryan, ApJ 606 (2004) 635.
- [39] C.L. Sarazin, preprint [astro-ph/0406193].
- [40] A. Raig, G. Gonzalez-Casado, E. Salvador-Sole, ApJ 508 (1998) L129.
E. Salvador-Sole, J.S. Solanes, A. Manrique, ApJ 499 (1998) 542.
- [41] E. Scannapieco, R.J. Thacker, ApJL 590 (2003) 69.
- [42] W.J. Percival, D. Scott, J.A. Peacock, J.S. Dunlop, MNRAS 338 (2003) L31.
- [43] M. White, ApJS 579 (2002) 16.
- [44] R. Yan, M. White, A. Coil, ApJ 607 (2004) 739.
- [45] M. Davis, G. Efstathiou, C.S. Frenk, S.D.M. White, ApJ 292 (1985) 371.
- [46] D.J. Eisenstein, P. Hut, ApJ 498 (1998) 137.
- [47] M. White, A&A 367 (2001) 27.
- [48] W. Hu, A.A. Kravtsov, ApJ 584 (2003) 702.
- [49] A.R. Liddle, D.H. Lyth, *Cosmological Inflation and Large-Scale Structure*, Cambridge University Press, Cambridge (2000)
- [50] A. Knebe, V. Muller, A & A 341 (1999) 1.
- [51] A. Nusser, R.K. Sheth, MNRAS 303 (1999) 685.
- [52] R.K. Sheth, G. Tormen, MNRAS 349 (2004) 1464.
- [53] P. Rosati, S. Borgani, C. Norman, ARA&A 40 (2002) 539 [astro-ph/0209035].